FT-8 2148F

STRESSES IN THE FIRST WALL OF A DUAL-COOLANT LIQUID-METAL BREEDER BLANKET DURING ELECTRON-BEAM WELDING

FIRST-WALL TECHNOLOGY

KEYWORDS: *welding blanket segments, welding stresses, residual stresses*

LEON CIZELJ *Jožef Stefan Institute, Reactor Engineering Division*
~~*P.O.B. 100, 61111 Ljubljana, Slovenia*~~
3000, 1000
HEINZ RIESCH-OPPERMANN *Forschungszentrum Karlsruhe*
Institut für Materialforschung II, P.O.B. 3640, 76021 Karlsruhe, Germany

Received April 5, 1996
Accepted for Publication July 24, 1996

Electron-beam (EB) welding is an important joining technique for fabricating and assembling blanket and first-wall components in fusion reactors. A numerical modeling of the EB procedure of a selected part of a DEMO fusion reactor blanket is presented. Stress and temperature distributions during and after EB welding are analyzed with the help of nonlinear finite element calculations, including phase transformations of MANET stainless steel. Residual stresses are discussed. Their magnitude and distribution may stimulate the initiation and growth of surface cracks parallel to the weld. Analysis of postweld heat treatment shows that the residual stresses can be neglected if appropriate postweld heat treatment is performed.

The main drawback of this analysis seems to be the lack of appropriate material data for high temperatures close to the melting point. Despite this, qualitative statements on the feasibility of joints are possible, and improved analyses of welding stresses are expected to make a valuable contribution to future studies that address the safety and reliability of blanket structures.

I. INTRODUCTION

The electron beam (EB)–welding procedure has several attractive properties: The heat input in the material is comparatively low, very precise fabrication is possible, and nondestructive (ultrasonic) examination of the welds is rather uncomplicated when compared with other welding procedures. This makes EB welding an attractive process for joining the different parts of the blanket and first wall in a DEMO fusion reactor, irrespective of the choice of the final design and the breeding and cooling media (for further information on blanket functions and designs, see, for example, Ref. 1). In this paper, we focus on the dual-coolant-blanket concept.[2] This is a self-cooled, liquid-metal breeder blanket with a helium-cooled first wall made of MANET martensitic stainless steel. The use of similar welds is also under consideration in other blanket concepts.

An important step in fabricating blanket segments is the joint between the poloidal sections of the box (see Fig. 1). According to safety and reliability criteria, no single welds between plasma and helium or liquid metal, respectively, are allowed. This suggests the use of an EB-welding procedure that is capable of producing a double weld in a single pass. The gap between the two welds additionally serves as part of a leak-detection system.

I.A. Objectives and Scope of the Paper

The lifetime of the blanket structure is expected to be governed by thermal fatigue in connection with the radiation-induced changes of the mechanical properties caused by operating the reactor. The useful life of the whole structure will be essentially defined by the useful life of the welds. We therefore initiated an analysis to estimate the temperatures and stresses during and after the welding. We consider estimating the residual stresses of welding in a complex geometrical shape to be a primary objective of our investigation. Our secondary objective has been to explore the potential of numerical simulation techniques to support forthcoming design feasibility and safety studies. Both objectives are further supported by the following facts:

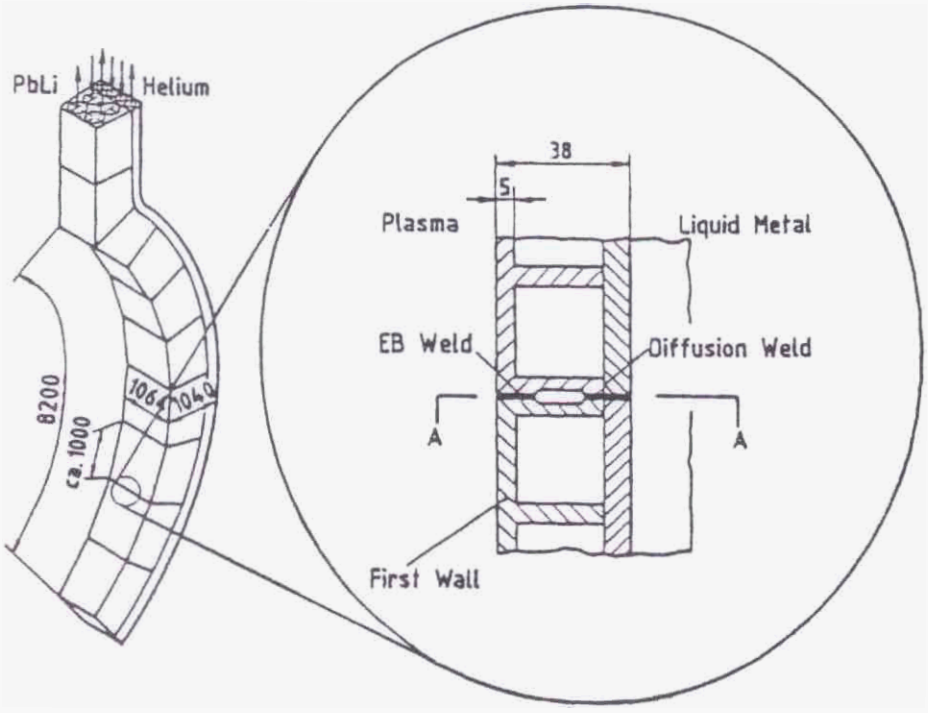

Fig. 1. Details of a double weld.

1. Only very limited experimental data on residual stresses caused by EB welding are available.[3]

2. There is a known tendency toward different forms of hot cracking[4] of EB-welded steels of all grades, which is accelerated by high-tensile strains during solidification.

3. Welded martensitic stainless steels are known to be prone to stress corrosion cracking (SCC) in air at room temperatures if subjected to tensile stresses (e.g., welding residual stresses).

The dual-coolant-blanket concept[2] is addressed by the present investigation, which is described in some detail in Ref. 5. Experience with this reference case facilitates generalization and addressing specific features of other design concepts.

I.B. A Survey of Computational Weld Mechanics

Considerable effort has already been devoted to the numerical simulation of welding. The main results sought by such simulations concern time-dependent temperature and displacement fields in welded specimens. Reviews of work already done are given in Refs. 6, 7, and 8.

Goldak et al.[7] suggested that the continuum mechanics can and should be directly applied to the analysis of welds. Further, the finite element method was suggested to be the most flexible and powerful tool. To date, it has already been applied to various problems, including conventional arc welding,[6] flame cutting of plates,[9] and heat treatment of surfaces by means of laser beams.[10] Goldak et al.[7] also identified some aspects that are typical for the weld mechanics. These include

1. richness of interaction between various phenomena (thermal, mechanical, and microstructural)
2. large range of analyzed temperatures (from room temperature to temperatures well above the melting point)
3. large range of length scales (details of the order of 1 mm or less in the workpieces of the order of 1 m or more should be analyzed).

Appropriate research of the foregoing specific points is essential to obtain reasonably accurate and computationally feasible solutions. Further, appropriate experimental support and verification of the simulation results is recommended.

I.C. Specifics of EB Welding

Electron-beam welding utilizes about three orders of magnitude higher power densities (10^{10} to 10^{13} W/m^2) than conventional-arc-welding procedures (10^6 to 10^8 W/m^2) (Ref. 11). Increasing the power density decreases the time for the heat obtained from the welding tool to be conducted into the workpiece. The consequence of concern to our analysis is a significantly faster and rather

localized thermal transient. Additionally, the vaporization of the welded metal significantly increases the range of temperatures to be analyzed. In summary, all aspects peculiar to weld mechanics (Sec. I.B) are even more pronounced in the case of EB welding. Therefore, in the absence of evidence to the contrary, the finite element methods used in the analysis of arc welding are considered adequate to be used as a first approximation of EB welding. This is in agreement with published practice.[12]

II. MODEL OF THE DOUBLE WELD

The following analysis employs a nonlinear transient solution of uncoupled thermal and displacement fields. The ABAQUS finite element–based code[13] was used in the analysis. Only the temperatures and displacements in the sections far away from the start/end of the weld were investigated. This was assumed in order to allow for the computationally more simple two-dimensional models.

II.A. Finite Element Mesh

A two-dimensional mesh was developed, as shown in Fig. 2. The weld was located in the y-z plane, which is also the plane of symmetry of the model. The assumption was made of solidification lines parallel to the y axis that might result in neglecting some rotations around the out-of-plane z axis. The details of the geometry are given in Ref. 5.

Generalized plane strain conditions were assumed in the stress analysis. This allowed for limited thermal expansion in the direction of the z axis. A linear variation over elements was assumed for temperatures and was quadratic for displacements. Stress analysis was carried out using hybrid elements with reduced integration. The thickness of the layer that we analyzed (z axis) was set to 1 mm. An approximation of the heat-affected zone (HAZ) was included in the model to enable us to simulate local phase transformations (see Sec. II.B). We manually generated the approximation using results of heat transfer analysis: All nodes where the temperature exceeded the austenitization temperature of 870°C were assumed to be members of HAZ (see Fig. 3).

II.B. Loading

The only loading considered in the analysis was the heat flux transmitted from the EB to the workpiece. The EB was modeled as a body heat source of appropriate uniform density. The heat source affected a 0.8-mm-wide layer of elements along the weld centerline (shaded in Fig. 2) to simulate the oscillatory motion (in the direction of x in Fig. 2) of the EB during welding. The heat source was suddenly turned on at the beginning of the analysis and completely turned off after 0.25 s. This time corresponds to the time needed by an EB with a velocity of 4 mm/s to pass the 1-mm-thick layer that we analyzed. This is based on the assumption that the diffusion of heat in the direction of welding is negligible compared with diffusion in the direction perpendicular to the weld.

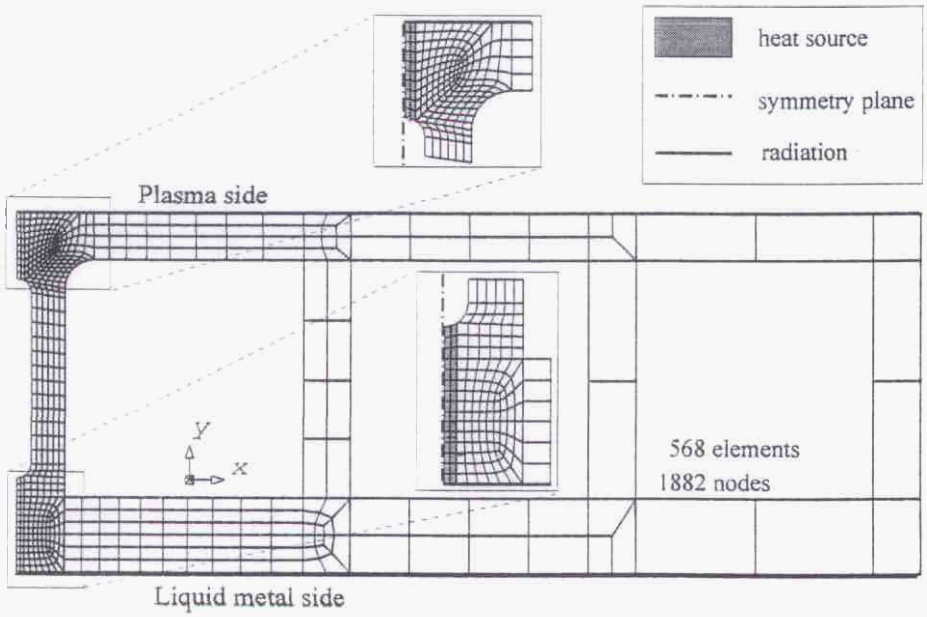

Fig. 2. Layout of the finite element mesh.

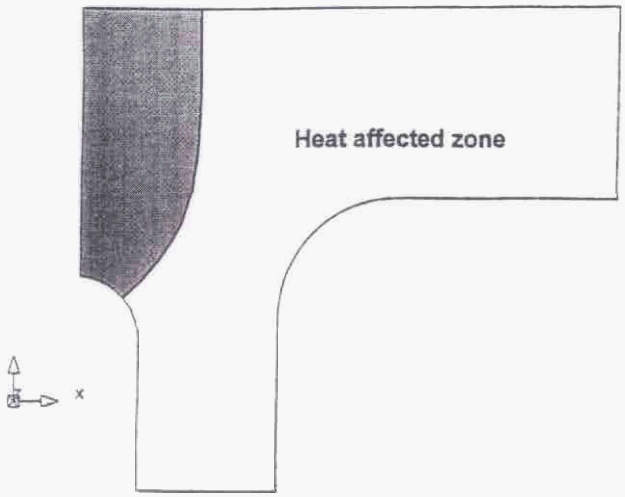

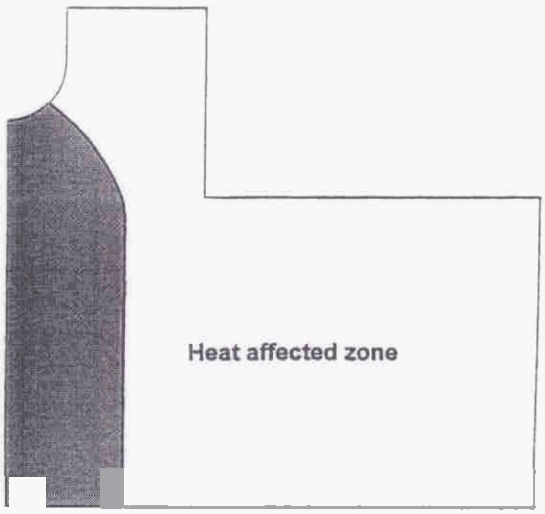

Fig. 3. Size and position of HAZ.

The heat losses of the workpiece in the vacuum chamber were modeled through thermal radiation with an emissivity of 0.5 on both free surfaces. Cavity radiation in the cooling channels was considered to be negligible, which is reasonable at the beginning of the transient but may result in slightly overestimated temperatures in the later stages of the transient. The temperature fields obtained by thermal analysis were used to generate thermal strains in the stress analysis. A cutoff temperature of 1000°C was introduced to maintain thermal strains at a constant level at higher temperatures (Fig. 4). This improved the numerical stability at higher temperatures where the tensile stiffness of the material was essentially vanishing. According to Näsström et al.,[14] the error in residual stresses caused by this simplification is of the order of 5%.

The heat treatment after the welding was modeled in the following way. A prescribed uniform temperature field was steadily increased from 20 to 760°C with an increase rate of 4°C/min. After a holding time of 2 h (at 760°C), uniform cooling at the rate of 4°C/min took place

II.C. Material Model

During the welding phase, a time-independent plasticity model with von Mises yield function, the associated flow rule, and isotropic hardening were assumed. All material parameters were assumed to be temperature dependent. The database on the material properties of the MANET martensitic stainless steel was sufficient to describe the behavior of the material up to ~700°C (Ref. 17). At temperatures close to the melting point, the parameters that describe strength (e.g., yield strength, and Young's and hardening moduli) were assumed to vanish while Poisson's ratio was set at 0.5. A relatively smooth transition was provided in the temperature range between 700°C and the melting point (consistent with data published by Karlsson[6]).

The constitutive laws valid for solid state were assumed to be valid in the entire range of temperatures analyzed. This was justified to some extent by the extremely small masses of molten and vaporized metal compared with the workpiece analyzed. Also note here that the constitutive models that we used essentially neglected many effects, which may be important at high temperatures (e.g., strain rate, dynamic recrystallization, different behavior in tension, and compression). The main reason leading to these assumptions is the lack of specific data that describe the response of material at high temperatures. Thus, the constitutive model is considered to be the weakest point of the present analysis and may significantly influence the accuracy of our results. However, the model and its results are considered to be at least qualitatively correct. Refined experimental support of the high-temperature behavior of the material is crucial in order to obtain more accurate results.

Creep was assumed to be the main residual stress relaxation mechanism during the postwelding heat treatment. A simple Norton creep was modeled, as supported by available data.[17]

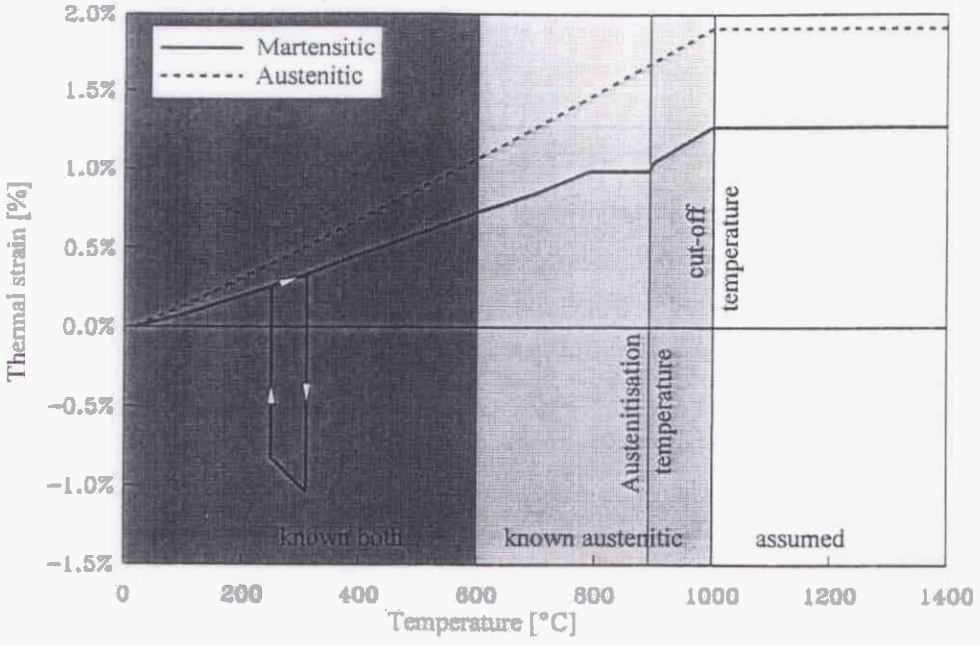

Fig. 4. Thermal strain and range of known material data for the martensitic (base material) and austenitic (HAZ) phases.

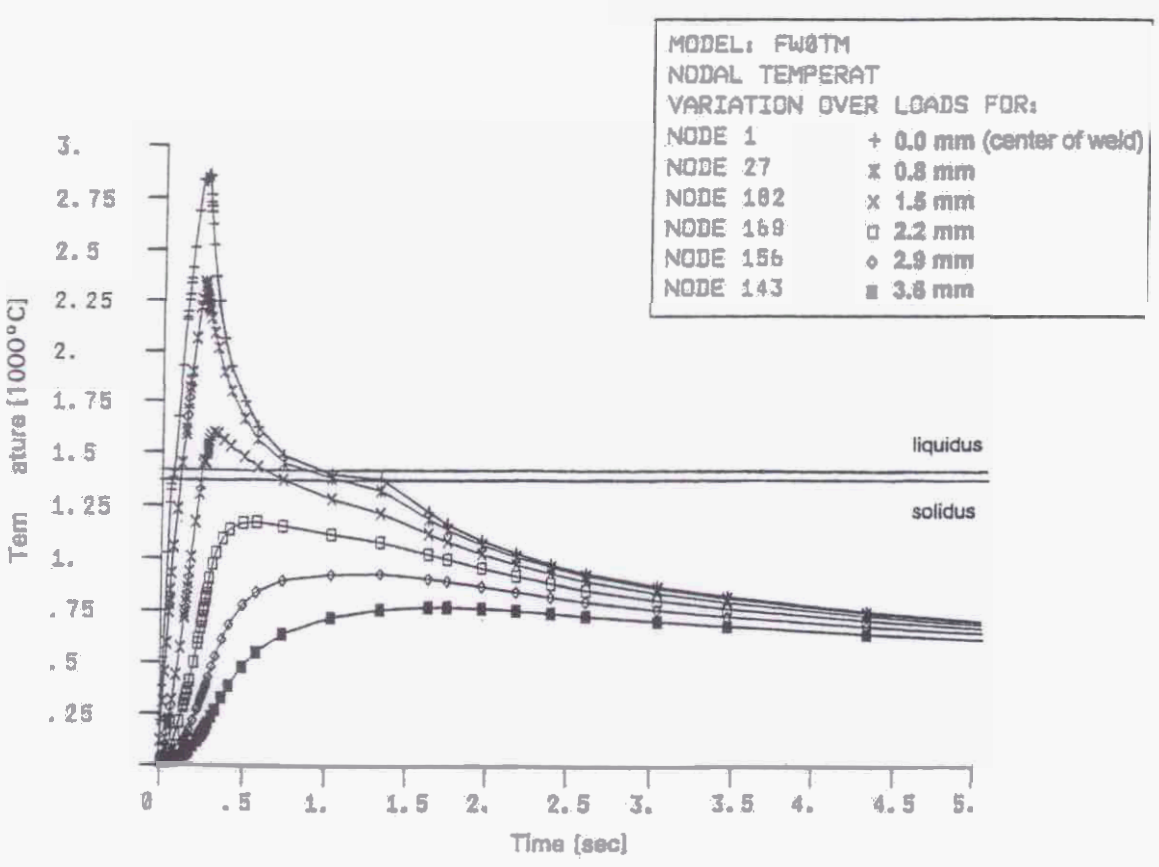

Fig. 5. Time history of temperatures in the vicinity of the weld (liquid-metal side).

III. RESULTS

Some selected results on temperatures, stresses, and residual stresses are given here. A more comprehensive discussion is given in Ref. 5.

III.A. Temperatures

A time history of the temperatures in the vicinity of the weld is shown in Fig. 5 as a function of the distance from the centerline of the weld. The distance was measured along the surface on the liquid-metal side of the weld (see Fig. 2). After the heat source was turned on, the melting point (1400°C) was reached in ~0.05 s. This may cause thermal strain rates of the order of 1/s. The vaporization temperature (~3000°C) was reached in ~0.2 s. At 0.25 s, the heat source was turned off, which caused cooling of the workpiece. The effect of latent heat is clearly shown as a plateau between 0.5 and 1.3 s.

The liquidus front propagated slightly more than 1.5 mm apart from the weld centerline. Temperatures at points located more than 3 mm from the weld centerline remained below 800°C. The time between the initiation of welding and final solidification was estimated to be ~1.5 s. The longest exposure to the temperatures exceeding the austenitization temperature was ~3 s. The time of cooling from 800 to 500°C ($\Delta t_{8/5}$) was 8.5 s.

The extent of the HAZ is shown in Fig. 3. Note here that about one-half of the load-carrying ligament between the welds was subjected to severe micromechanical changes. This may have affected its load-carrying capabilities. The spatial distribution of temperatures at 0.267 s (0.017 s after the heat source was turned off) is shown in Fig. 6. The parallel and rather dense isotherms show rather localized heat conduction and virtually negligible radiation fluxes at this early stage of the thermal transient.

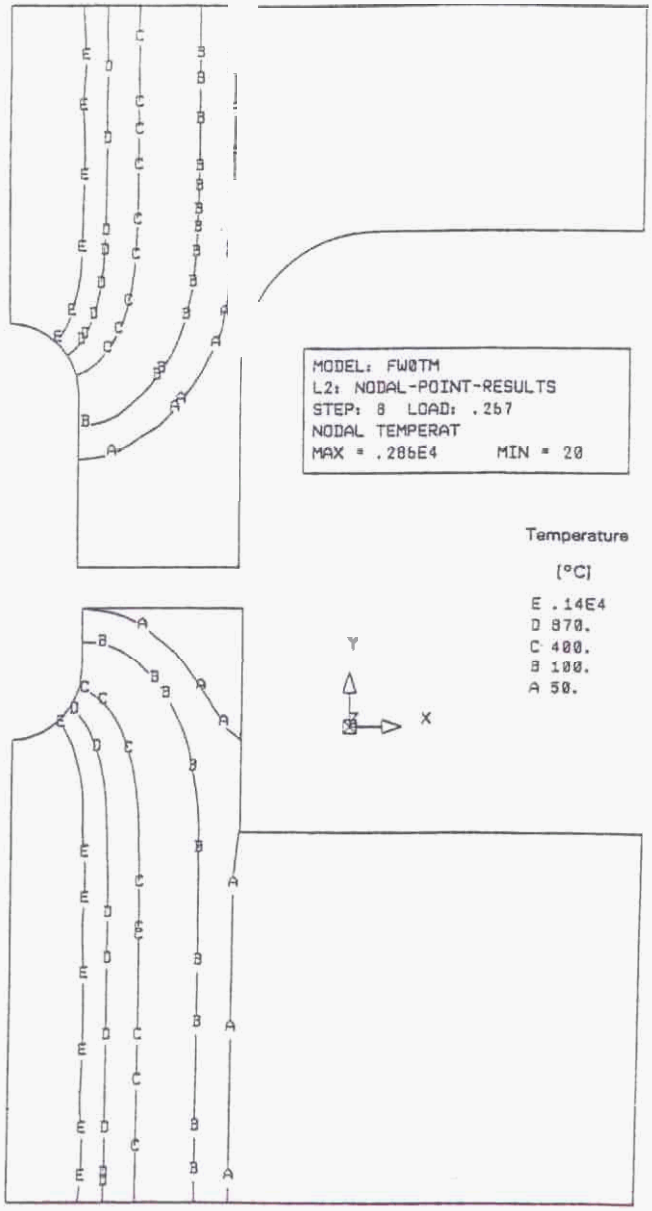

Fig. 6. Spatial distribution of temperatures (heat source turned off); time = 0.267 s.

III.B. Stresses During Welding

The stresses that developed during welding were of course a strong function of time. It is beyond the scope of this paper to give a full development. A typical pattern of equivalent von Mises stresses is, however, given in Fig. 7. The majority of the stresses that developed during welding were concentrated in a very narrow zone close to the weld centerline. The highest stresses exceeded the yield strength during the entire thermal transient.

III.C. Residual Stresses

The residual stresses presented here were obtained as steady-state stresses following a complete time-dependent simulation of the welding stresses. Only the transverse (in the direction of the x axis) residual stresses are addressed in this paper (Fig. 8) because those stresses tend to accelerate the cracks that are parallel to the weld and are therefore the most significant component of residual stresses.

The range of transverse residual stresses was rather large: from −500 to 860 MPa, which exceeds the yield strength of the material at room temperature (614 MPa). This should be at least partially attributed to the rather crude simulation of the volume expansion during austenite to martensite transformation. The tensile residual stresses tended to concentrate at both surfaces of the first wall and at the leak-detection slot. Such distribution and magnitude of stresses combined with a rough surface inside the leak-detection slot may enhance the initiation

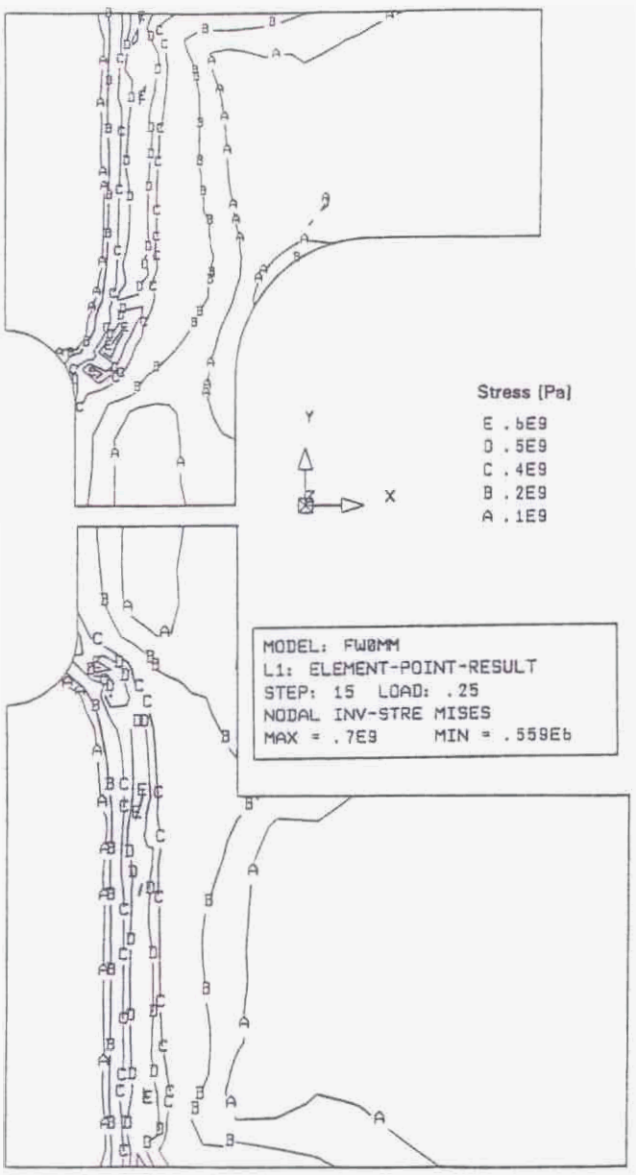

Fig. 7. Equivalent von Mises stresses during heatup (0.25 s, plasma side weld up, liquid-metal side weld down).

and propagation of fatigue or stress corrosion cracks. Such problems, especially air-assisted SCC, which is typical for martensitic steels, may be significantly reduced by relieving the stress immediately after the welding.

III.D. Postwelding Heat Treatment

Relaxation of the residual stresses during the postwelding heat treatment was modeled through creep. Simple Norton creep was utilized, as supported by the available material database. The thermal cycle simulated is described in Sec. II.B. The relaxation of equivalent (von Mises) residual stress with increasing temperature is shown in Fig. 9 together with the yield strength of the base material before welding. Note here that the majority of residual stresses vanished during the heatup phase. The final value of the equivalent (von Mises) residual stress was estimated to be of the order of 1 MPa, which is considered negligible.

IV. CONCLUSIONS

The primary task of the research presented in this paper was to analyze the residual stresses in an EB-welded double weld of a dual-coolant, liquid-metal

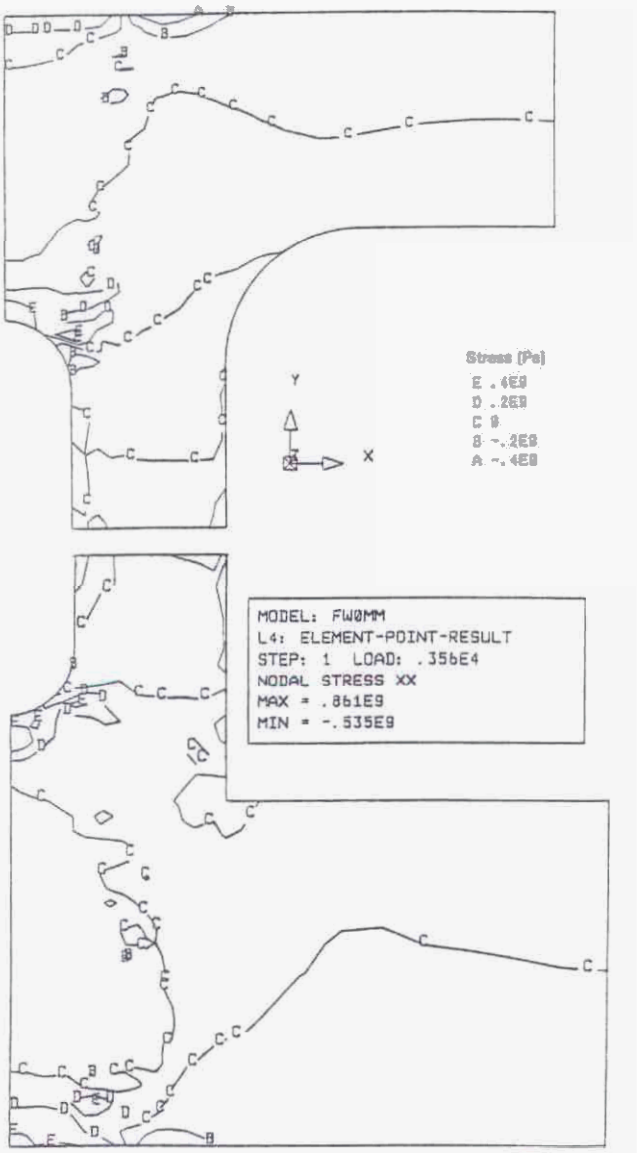

Fig. 8. Transverse (σ_{xx}) residual stresses (plasma side weld up, liquid-metal side weld down).

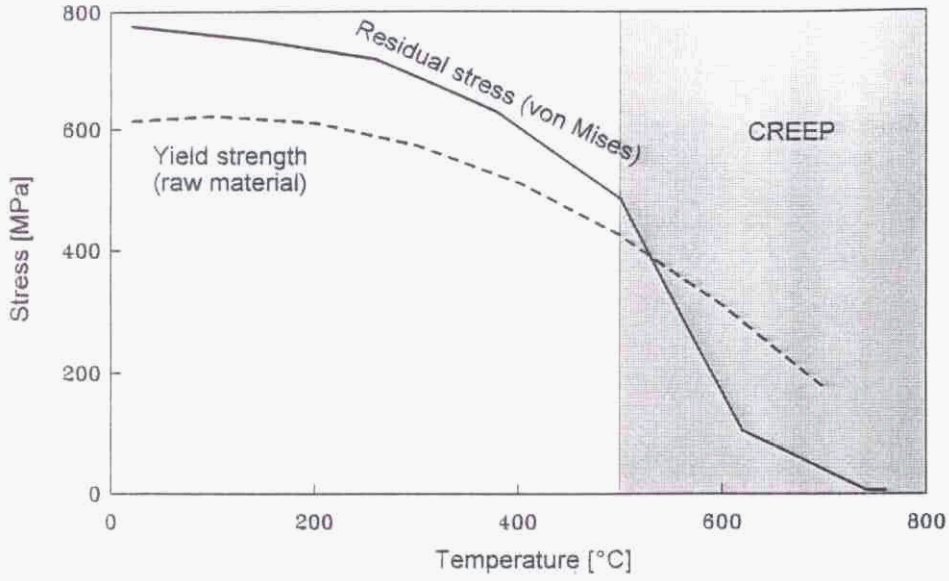

Fig. 9. Relaxation of residual stresses during postwelding heat treatment.

breeder-blanket segment. A nonlinear finite element solution of the uncoupled thermal and displacement fields was utilized. Our results mainly concerned time-dependent temperature and stress fields, but, we also obtained distributions of residual stresses. The magnitude (up to 860 MPa) and distribution of tensile residual stresses may stimulate the initiation and growth of surface cracks parallel to the weld, at both the surfaces and inside the leak-detection slot. A special concern may be air-assisted SCC, which is typical for martensitic steels. We also analyzed postwelding heat treatment. The results indicate that residual stresses vanish during the heatup phase. Thus, residual stresses may be neglected if appropriate postwelding heat treatment is performed.

Our results provide useful information about the welding process as well as important hints about the fabrication feasibility of geometrical configurations as proposed by different design concepts. The constitutive model, which is limited by a lack of data on high-temperature behavior, is considered to be the weakest point of the present analysis. This may significantly influence the accuracy of our results. However, we consider the model and its results to be at least qualitatively correct. Experimental support in the future is necessary in order to obtain more accurate results. Improved analyses of welding stresses are expected to make a considerable contribution to future studies that address the safety and reliability of blanket structures.

ACKNOWLEDGMENTS

This research was performed during the guest scientist mission of L. Cizelj at Kernforschungszentrum Karlsruhe, Institut für Materialforschung II between November 1, 1993 and April 30, 1994. This mission was supported by the Projekt Kernfusion.

The valuable discussions with and comments by E. Diegele are gratefully acknowledged.

REFERENCES

1. H. JOHN, S. MALANG, and H. SEBENING, "DEMO-Relevant Test Blankets for NET/ITER, Part 1: Self-Cooled Liquid Metal Breeder Blanket," Vol. 2, KfK-4908, Kernforschungszentrum Karlsruhe (1991).

2. S. MALANG, E. BOJARSKY, L. BÜHLER, H. DECKERS, U. FISCHER, P. NORAJITRA, and H. REISER, "Dual Coolant Liquid Metal Breeder Blanket," *Proc. 17th Int. Symp. Fusion Technology (SOFT)*, Rome, Italy, September 14-18, 1992, Vol. 2, p. 1424, C. FERRO, Ed., Elsevier.

3. R. POJE, "Schweisseigenspannungen in Elektronenstrahl- und Unterpulver-Schweissverbindungen von Stählen bei verschiedenen Blechdicken," Dissertation (1984).

4. Y. TOMITA, K. TANABE, and K. KOYAMA, "Improving Toughness of Electron Beam Welds of Heavy Mn-Mo-Ni Steel Plates for Pressure Vessels," *J. Pressure Vessel Technol.*, **115**, 242 (1993).

5. L. CIZELJ and H. RIESCH-OPPERMANN, "An Analysis of Electron Beam Welds in a Dual Coolant Liquid Metal Breeder Blanket," KfK-5360, Kernforschungszentrum Karlsruhe (1994).

6. L. KARLSSON, "Thermal Stresses in Welding," *Thermal Stresses Vol. 1*, p. 299, R. B. HETNARSKI, Ed., North Holland Publishing Company, Amsterdam (1986).

7. J. GOLDAK, A. ODDY, M. GU, W. MA, A. MASHAIE, and E. HUGHES, "Coupling Heat Transfer, Microstructure Evolution and Thermal Stress Analysis in Weld Mechanics," *Mechanical Effects in Welding*, p. 1, L. KARLSSON, L.-E. LINDGREN, and M. JONSSON, Eds., Springer-Verlag, New York (1992).

8. K. MASUBUCHI, *Analysis of Welded Structures*, Pergamon Press, New York (1980).

9. L. E. LINDGREN, A. CARLESTAM, and M. JONSSON, "Computational Model of Flame-Cutting," *J. Eng. Mater. Technol.*, **115**, 440 (1993).

10. J. M. BERGHEAU, D. PONT, and J. L. LEBLOND, "Three-Dimensional Simulation of a Laser Surface Treatment Through Steady State Computation in the Heat Source's Comoving Frame," *Mechanical Effects in Welding*, p. 85, L. KARLSSON, L.-E. LINDGREN, and M. JONSSON, Eds., Springer-Verlag, New York (1992).

11. M. B. C. QUIGLEY, "High Power Density Welding," *Physics of Welding*, 2nd ed., J. F. LANCASTER, Ed., Pergamon Press, New York (1986).

12. J. GOLDAK, A. CHAKRAVARTI, and M. BIBBY, "A New Finite Element Model for Welding Heat Sources," *Metall. Trans.*, **15B**, 299 (1984).

13. "ABAQUS Users Manual," Ver. 4.9, Hibbit, Karlsson, and Sorrensen.

14. M. NÄSSTRÖM, L. WIKANDER, L. KARLSSON, and L. E. LINDGREN, "Combined Solid and Shell Element Modelling of Welding," *Mechanical Effects in Welding*, p. 197, L. KARLSSON, L.-E. LINDGREN, and M. JONSSON, Eds., Springer-Verlag, New York (1992).

15. K. KUSSMAUL, E. ROOS, and W. GUTH, "A Contribution to the Numerical and Experimental Determination of Residual Stresses in Welds," *Nucl. Eng. Des.*, **112**, 337 (1989).

16. A. M. DONORE and F. WAECKEL, "Influence des transformations structurales dans les lois de comportement élastoplastiques," HI-74/93/024, Electricité de France (1993).

17. M. KÜCHLE, "Material Data Base for the NET Test Blanket Design Studies," First Draft, Kernforschungszentrum Karlsruhe (1988).

Physics

Leon Cizelj (PhD, ~~nuclear~~ engineering, University of Ljubljana, Slovenia) is a research associate in the Reactor Engineering Department of Jožef Stefan Institute, Ljubljana. His research interests include structural analysis and probabilistic fracture mechanics.

Heinz Riesch-Oppermann (PhD, mechanical engineering, University of Karlsruhe, Germany) is a scientist in the Institute for Materials Research at Forschungszentrum Karlsruhe. His current research areas are reliability engineering, probabilistic fracture mechanics, and stochastic modeling of material behavior.